Uzbekistan Journal of Polymers
journal homepage: https://uzpolymerjournal.com/
ISSN (online): 2181-3256 (print) 2181-3248

OPTIMIZATION OF THE SYNTHESIS OF SULFUR CELLULOSE COMPOSITES BY INVERSE VULCANIZATION: INFLUENCE OF TEMPERATURE, TIME, AND COMPONENT RATIO

Saydullo Kh. Azimov[1], Umida R. Baltayeva[2], Umida Kh. Asranova[3]

[1] *"NEFTGAZ-MALAKA" Training and Research Center, JSC "O'ZLITINEFTGAZ", Tashkent, Uzbekistan*
[2] *National University of Uzbekistan, Tashkent*
[3] *Andijan State Technical Institute, Andijan, Uzbekistan*

ARTICLE INFO

Received:27April 2026
Revised: 12 May 2026
Accepted: 12 June 2026

Keywords:
inverse vulcanization; sulfur-cellulose composite; Box-Behnken design; thermal stability; drilling fluid additive; waste valorization; FTIR spectroscopy

Corresponding author
baltayevaumida31@gmail.com

ABSTRACT

This article presents the optimization of sulfur-cellulose composite (SCC) synthesis via inverse vulcanization using waste elemental sulfur (S_8) and activated cotton husk. A three-factor Box-Behnken design was applied (factors: temperature 160-190°C, time 90-180 min, S:Org mass ratio 40:60-60:40). Regression models were built for three responses: product yield (Y_1), onset decomposition temperature (Y_2, T_{onset}), and fluid loss reduction efficiency (Y_3). All three factors significantly affect composite properties, with temperature being dominant. Optimal synthesis conditions were: T = 185°C, τ = 135 min, S:Org = 55:45. Under these conditions, the composite exhibited a yield of 91.8%, T_{onset} = 272°C, and fluid loss reduction of 62.5%. The use of a catalyst (hexamethylenetetramine, 1 wt% of sulfur) increased yield by 6.6% and thermal stability by 24°C compared to non-catalyzed synthesis. The composite was characterized by FTIR, TGA, XRD, and SEM-EDX, confirming its formation. The obtained composite is recommended as a thermostable additive for drilling fluids at temperatures up to 180°C.

DOI: *10.66640/UJP-2026-5-00009*

Introduction

The drilling of deep high-temperature high-pressure (HTHP) wells requires fluid loss additives that maintain rheological and filtration properties at temperatures up to 180-200°C [1,2]. Conventional cellulose derivatives (carboxymethyl cellulose, CMC; polyanionic cellulose, PAC) and synthetic polymers (polyacrylamides) undergo hydrolytic and thermal degradation already at 150-160°C, leading to loss of viscosity and increased fluid loss [3,4]. Although crosslinked and modified celluloses show improved thermal stability, most commercial additives fail above 180°C, creating a demand for new thermostable materials.

Several chemical modification strategies for cellulose have been explored to enhance thermal stability and functional properties, including esterification, etherification, and graft copolymerization [5,6]. However, these methods often require expensive reagents, multistep synthesis, and organic solvents, and the resulting products may still degrade under HTHP conditions. A promising alternative is inverse vulcanization - a one-step reaction of molten

elemental sulfur with organic comonomers that produces stable polysulfide polymers [7,8]. This method not only valorizes waste sulfur but also enables the incorporation of biomass-derived components, including lignin, vegetable oils, and cellulose [9,10].

The mechanism of inverse vulcanization involves thermal homolytic ring-opening of cyclooctasulfur (S_8) above 159°C, generating diradical sulfur species. These radicals polymerize into long polysulfide chains $(-S-S-)_n$, which then react with unsaturated or hydroxyl-containing organic monomers via C-S bond formation. In the case of cellulose, the primary hydroxyl groups ($-CH_2OH$) can attack the polysulfide chains, forming thioether linkages (-C-S-) and generating a crosslinked sulfur-cellulose network. A schematic representation of this mechanism is shown in the following diagram.

Step 1. *Ring-opening of sulfur:* $S_8 \xrightarrow{160-190°C} \bullet S\text{-}S\text{-}S\text{-}S\text{-}S\text{-}S\text{-}S\text{-}S\bullet$

Step 2. *Formation of polysulfide chains:* $n\ S_8 \xrightarrow{heat} \bullet(S)_n\ \bullet$

Step 3. *Reaction with cellulose hydroxyl groups: Cell-OH +* $\bullet(S)_n\bullet \rightarrow$ *Cell-O-*$S_n\bullet$

Step 4. *Crosslinking: Cell-O-*$S_n\bullet$ + $\bullet S_m$*-O-Cell →* *Cell-O-*S_{n+m}*-O-Cell*

Result: *Three-dimensional sulfur-cellulose network*

Uzbekistan faces two large-scale waste streams: elemental sulfur from gas processing plants (hundreds of thousands of tons annually) and cotton husk from the textile industry (>400,000 t/year) [11,12]. Previously, we developed an alkaline activation method for cotton husk that increases the cellulose content to 50-55% and improves the accessibility of hydroxyl groups [13]. Inverse vulcanization of activated cotton husk with waste sulfur offers a low-cost, environmentally friendly route to thermostable composites. However, to obtain reproducible and application-oriented properties, a systematic optimization of synthesis parameters (temperature, time, and component ratio) is required. Recent studies in the Uzbekistan Journal of Polymers have highlighted the potential of local raw materials for functional polymer composites [14,15], but no work has yet applied response-surface methodology to sulfur-cellulose systems.

The aim of this work is to establish quantitative relationships between inverse vulcanization parameters (temperature, time, S:Org mass ratio) and the key properties of sulfur-cellulose composites - product yield, thermal stability (T_{onset} from TGA), and fluid loss reduction efficiency in drilling fluids. Using a Box-Behnken design, we determine optimal synthesis conditions and compare the performance of the optimized composite with commercial additives (CMC, PAC). The results provide a basis for developing a thermostable drilling fluid additive from locally available waste.

Materials and Methods. The following materials and reagents were used: technical sulfur (S_8) from the Mubarek Gas Processing Plant (Uzbekistan), conforming to GOST 127.1-93 [16]; cotton husk - a waste product of cotton ginning plants in Tashkent region, activated according to the previously described method [9]; sodium hydroxide (NaOH), analytical grade, GOST 4328-77 [17]; hydrochloric acid (HCl), analytical grade, GOST 3118-77 [18]; distilled water, GOST 6709-72 [19]; hexamethylenetetramine (urotropine), GOST 1381-73 [20]; bentonite for drilling fluids, GOST 28177-89 (API 13A grade) [21]; potassium chloride (KCl), analytical grade.

Raw material pretreatment. Cotton husk was ground in a rotor mill to a particle size of 1-3 mm and subjected to alkaline activation according to method [9]: treatment with 5% NaOH solution (GOST 4328-77 [17]) at 80°C for 2 h (solid : liquid = 1:10), followed by washing with distilled water (GOST 6709-72 [19]) to neutral pH and drying at 80°C. The cellulose content in the activated husk was determined by the Kurschner-Hanak method (GOST 6840-78) [22] and found to be 53.6 wt.%.

Synthesis of sulfur-cellulose composites (SCC). The synthesis was carried out in a 500 mL three-neck flask equipped with a mechanical stirrer, reflux condenser, thermocouple, and nitrogen inlet. Sulfur and activated husk were loaded in a predetermined mass ratio (40:60, 50:50, or 60:40). An inert atmosphere was created with nitrogen (50 mL/min), and the mixture was heated to 130°C and held for 30 min. The temperature was then raised to the target value (160, 175, or 190°C), the

catalyst (hexamethylenetetramine, 1 wt.% relative to sulfur mass, GOST 1381-73 [20]) was added, and the reaction mixture was held for the required time (90, 135, or 180 min). After cooling to room temperature, the product was ground and sieved through a 75 μm mesh sieve (GOST 3584-73) [23]. The product yield was determined gravimetrically.

Determination of free and bound sulfur content. Free (unreacted) sulfur was extracted from the SCC samples using a Soxhlet apparatus with toluene as solvent. Approximately 2 g of ground SCC (75 μm) was placed in a cellulose thimble and extracted with 150 mL of toluene at 110°C for 8 h. The residue was dried at 60°C under vacuum to constant weight. The free sulfur content (wt.%) was calculated gravimetrically. The bound sulfur content was determined by elemental analysis of the extracted residue. All measurements were performed in duplicate. The extraction procedure corresponds to the classical description [24] (Vogel, A.I. Textbook of Quantitative Chemical Analysis).

Physicochemical characterization. Elemental composition (C, H, N, S) was determined using a EuroVector EA3000 microanalyzer according to the manufacturer's protocol [25].

FTIR spectra were recorded on a Shimadzu IRTracer-100 spectrometer in the range 400-4000 cm^{-1} (ATR mode, resolution 4 cm^{-1}, 32 scans). The spectra were processed using Shimadzu LabSolutions IR software [26].

X-ray diffraction (XRD) was performed on a Bruker D8 Advance diffractometer (CuKα radiation, λ = 1.5406 Å, 40 kV, 40 mA) in the 2θ range of 5-70° with a step size of 0.02° and a counting time of 0.5 s per step. Phase identification was carried out using the ICDD PDF-2 database [27].

Surface morphology and elemental distribution were studied using a JEOL JSM-IT300 scanning electron microscope equipped with an energy-dispersive X-ray (EDX) detector. Samples were sputter-coated with gold (10-15 nm thickness) prior to imaging. Micrographs were taken at accelerating voltages of 10-20 kV [28].

Thermal analysis was performed on a NETZSCH STA 449 F3 Jupiter synchronous thermal analyzer. Samples (≈10 mg) were heated from 30°C to 600°C at a rate of 10°C/min under nitrogen atmosphere (50 mL/min). The onset decomposition temperature (T_{onset}) was determined according to GOST R 56721-2015 [29] as the intersection of the baseline and the tangent to the thermogravimetric (TG) curve at the point of maximum weight loss.

Preparation and testing of drilling fluids. Model drilling fluids were prepared based on 3 wt.% bentonite (GOST 28177-89 [21]) in distilled water with the addition of 3 wt.% KCl and pH adjustment to 9.5-10.0 using NaOH solution. The SCC additive was introduced at a concentration of 2 wt.% relative to the water phase mass. Preparation was performed according to API RP 13B-1 (2019 edition) [30] using a high-speed mixer (Hamilton Beach, 12,000 rpm) for 20 min.

Rheological parameters - plastic viscosity (PV) and yield point (YP) - were measured on a FANN 35SA rotational viscometer at 25°C following API RP 13B-1 [30]. Gel strength (GS) was determined as the maximum dial reading 10 s and 10 min after the sample was allowed to rest.

Filtration characteristics under standard conditions were determined using an API filter press (Fann Instruments) at 100 psi (0.69 MPa) and room temperature (25±2°C) for 30 min. The filtrate volume (FL) was measured to the nearest 0.1 mL. The fluid loss reduction efficiency (Y_3) was calculated using the formula:

$$Y_3 = \frac{FL_{control} - FL_{experiment}}{FL_{control}} \cdot 100\%$$

where $FL_{control}$ is the filtrate of the base bentonite fluid without additive, and $FL_{experiment}$ is the filtrate of the fluid containing 2% SCC.

Experimental design and statistical analysis. A three-factor rotatable Box-Behnken design [31] was used for optimization. The factors and their coded levels are given in Table 1. The design included 12 factorial points and 3 center point replicates (total 15 experiments).

Table 1

Factors and coded levels

Code	Factor	Unit	Coded levels		
			-1	0	+1
X_1 (A)	Temperature	°C	160	175	190
X_2 (B)	Time	min	90	135	180
X_3 (C)	S:Org ratio	mass	40:60	50:50	60:40

Regression models and analysis of variance (ANOVA) were performed using Design-Expert 13 software. Coefficient significance was assessed at a 95% confidence level ($p < 0.05$). Model adequacy was checked using Fisher's F-test. The desirability function approach [31] (ibid., Montgomery) was used to determine the compromise optimum maximizing all three responses simultaneously.

Results and Discussion

The Box-Behnken design (15 experiments) yielded the results presented in Table 2.

Table 2

Design matrix and experimental results

Run	X_1 (T, °C)	X_2 (τ, min)	X_3 (S:Org)	Y_1 (%)	Y_2 (T_{onset}, °C)	Y_3 (%)
1	160	90	50:50	86.2	218	32.5
2	190	90	50:50	91.5	261	58.1
3	160	180	50:50	88.7	225	38.0
4	190	180	50:50	93.1	275	65.4
5	160	135	40:60	82.5	205	25.8
6	190	135	40:60	90.3	255	52.3
7	160	135	60:40	89.4	240	45.2
8	190	135	60:40	94.8	285	68.9
9	175	90	40:60	87.9	235	40.1
10	175	180	40:60	89.0	245	43.5
11	175	90	60:40	92.4	272	62.0
12	175	180	60:40	93.7	279	66.7
13	175	135	50:50	90.5	265	57.0
14	175	135	50:50	90.8	267	56.5
15	175	135	50:50	90.2	263	57.8

Note: Y_1 - product yield (%), Y_2 - onset decomposition temperature (°C), Y_3 - fluid loss reduction efficiency (%). Runs 13-15 are center point replicates

ANOVA showed that all three factors significantly affect product yield (Y_1), onset decomposition temperature (Y_2, T_{onset}), and fluid loss reduction efficiency (Y_3), with temperature being the dominant factor (F-values for Y_2: temperature 293.4, S:Org ratio 104.0, time 13.4). Pairwise interactions were not significant ($p > 0.05$). The regression models in coded variables are:

$$Y_1 = 90.50 + 2.08X_1 + 0.42X_2 + 1.67X_3 \ (R^2 = 0.945)$$
$$Y_2 = 265.20 + 15.75X_1 + 3.36X_2 + 9.38X_3 - 6.12X_1^2 \ (R^2 = 0.984)$$
$$Y_3 = 57.10 + 8.35X_1 + 1.15X_2 + 6.50X_3 \ (R^2 = 0.960)$$

All models were adequate ($p < 0.0001$, lack of fit not significant). Using the desirability function, the compromise optimum was found at: temperature = 185°C, time = 135 min, S:Org mass

ratio = 55:45. Predicted responses at the optimum: yield = 91.8%, T_{onset} = 272°C, fluid loss reduction = 62.5% (overall desirability D = 0.89).

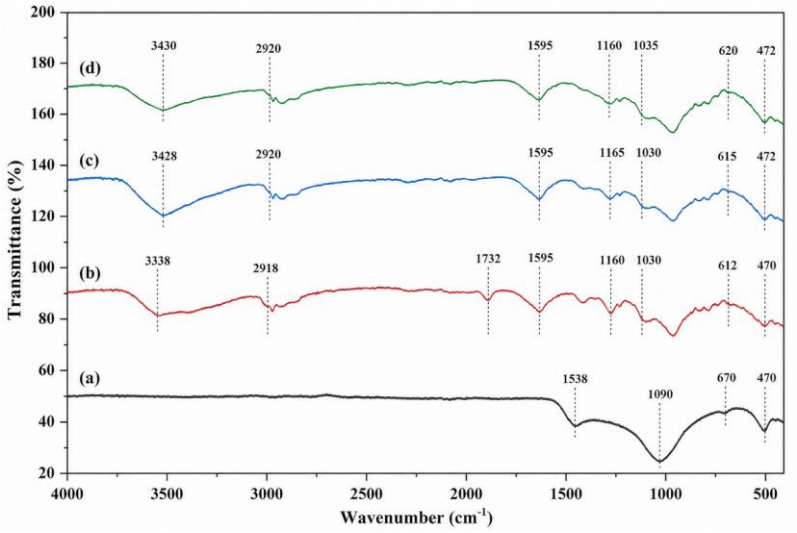

Figure 1. *FTIR spectra of (a) elemental sulfur, (b) activated cotton husk, (c) SCC without catalyst, (d) SCC with catalyst (optimum conditions).*

Figure 1 shows the FTIR spectra of the starting materials and the SCC samples. The spectrum of activated cotton husk exhibits broad O-H stretching vibrations at 3200-3400 cm^{-1}, C-H stretches at 2900-2920 cm^{-1}, and C-O-C glycosidic bridge vibrations at 1050-1150 cm^{-1}, characteristic of cellulose. Elemental sulfur shows no distinct bands in the mid-IR region, as expected.

The SCC spectra (both with and without catalyst) display the same cellulose-related bands, indicating that the cellulose backbone is preserved. A weak but reproducible band appears at 420 cm^{-1}, which has been tentatively assigned to C-S stretching vibrations, possibly corresponding to thioether linkages. This band is more intense in the catalyst-containing sample. However, FTIR alone cannot distinguish between covalent C-S bonds and physically mixed polysulfides; therefore, the presence of a band at 420 cm^{-1} and the absence of the S-S band are consistent with but do not prove the formation of covalent sulfur-cellulose linkages.

However, FTIR alone cannot distinguish between covalent C-S bonds and physically mixed polysulfides; therefore, the presence of a band at 420 cm^{-1} and the absence of the S-S band are consistent with but do not prove the formation of covalent sulfur-cellulose linkages. Complementary evidence from sulfur extraction (Section 3.6) and TGA (Section 3.3) is needed.

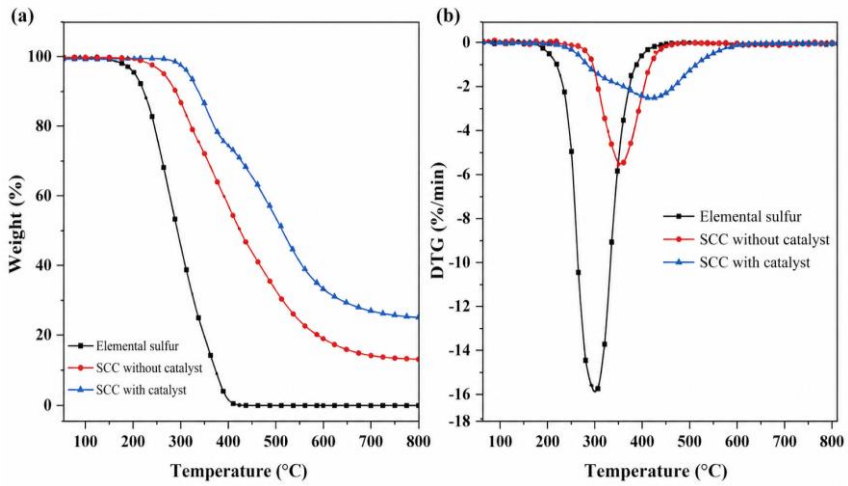

Figure 2. *(a) TGA and (b) DTG curves of SCC without catalyst, SCC with catalyst, and elemental sulfur*

Thermogravimetric analysis (Figure 2) reveals distinct decomposition behavior. Elemental sulfur shows a single sharp weight loss starting at ≈250°C (maximum rate at 280°C) due to evaporation. The SCC without catalyst exhibits a two-step degradation: an initial weight loss (≈5-8%) below 200°C attributed to residual moisture and low-molecular-weight species, followed by a major decomposition onset (T_{onset}) at 248°C. The SCC with catalyst shows a higher T_{onset} of 272°C and a reduced initial weight loss, indicating better thermal stability. The residual mass at 600°C (≈15-20%) corresponds to char and inorganic residues.

The shift of the main decomposition to higher temperatures in the catalyst-containing composite suggests stronger incorporation of sulfur into the cellulose matrix, possibly through more extensive crosslinking. Nevertheless, TGA cannot directly distinguish between chemically bound sulfur and finely dispersed free sulfur; this distinction is addressed by extraction (Section 3.6).

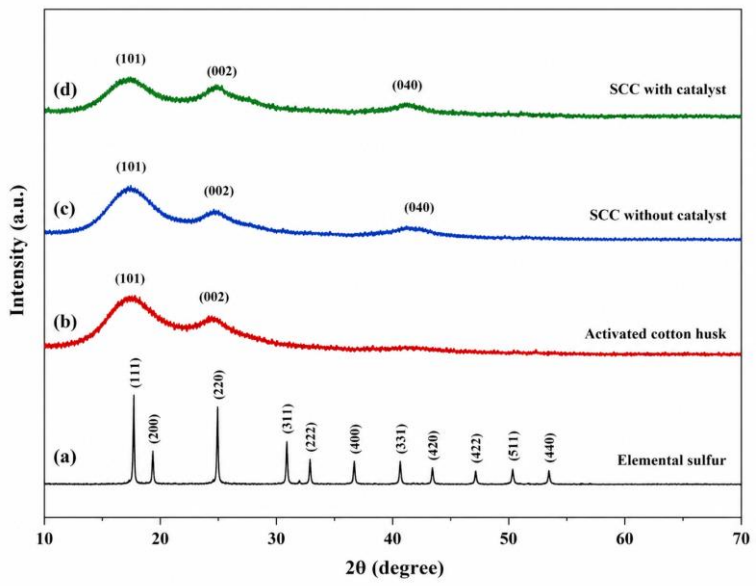

Figure 3. *XRD patterns of (a) elemental sulfur, (b) activated cotton husk, (c) SCC without catalyst, (d) SCC with catalyst.*

Figure 3 presents the XRD diffractograms. Elemental sulfur shows sharp crystalline peaks at 2θ = 23.1°, 25.8°, 27.7°, etc., corresponding to orthorhombic α-sulfur (ICDD 00-008-0247). Activated cotton husk exhibits the typical cellulose I pattern with broad peaks at 2θ ≈ 16° and 22.5°. The SCC samples display a predominantly amorphous halo with only weak residual sulfur peaks, indicating that most of the sulfur is either reacted or amorphously dispersed. The catalyst-containing sample shows even less crystalline sulfur, suggesting more efficient consumption of S_8 during the inverse vulcanization.

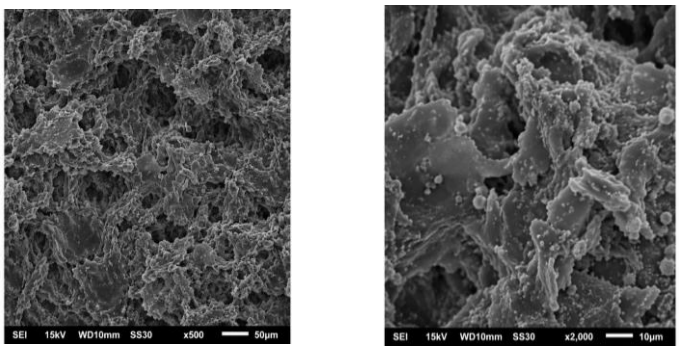

(a) (b)

Figure 4. *SEM micrographs of SCC (optimum conditions, with catalyst) at (a) ×500 and (b) ×2000 magnification.*

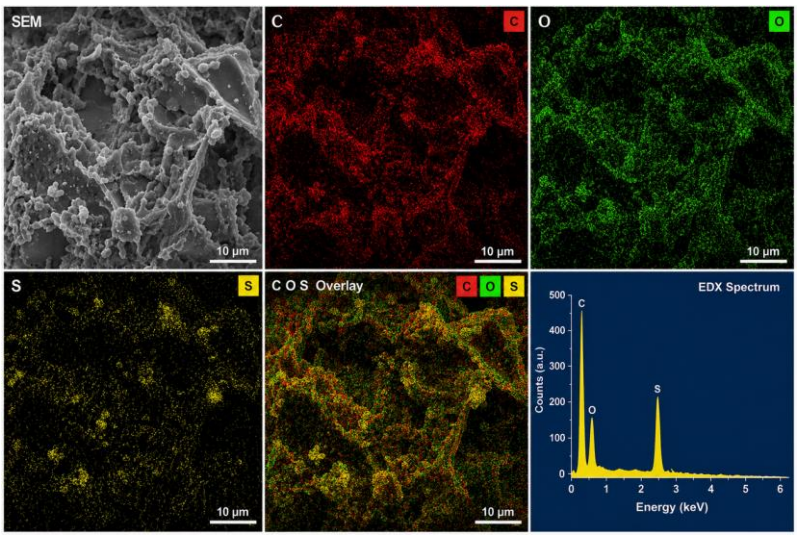

Figure 5. *EDX elemental maps (C, O, S) overlay for the same SCC sample.*

Scanning electron microscopy (Figure 4) reveals that the SCC consists of irregular particles (10-50 µm) with a rough, porous surface. No large separate sulfur crystals are visible, indicating homogeneous dispersion of sulfur within the cellulose matrix.

EDX mapping (Figure 5) shows that carbon, oxygen, and sulfur are uniformly distributed over the analyzed area, without sulfur-rich agglomerates. The average sulfur content by EDX (≈36 wt%) agrees well with the nominal composition (S:Org = 55:45 gives ≈42 wt% sulfur, but EDX is semi-quantitative). The uniform distribution supports the formation of an intimate composite, though it does not prove covalent bonding.

Table 3

Free and bound sulfur content in SCC samples (optimum conditions)

Sample	Free S (wt%)	Bound S (wt%)	Total S (wt%)
SCC without catalyst	12.3 ± 0.8	31.2 ± 0.6	43.5
SCC with catalyst (1% HMTA)	6.1 ± 0.5	38.4 ± 0.5	44.5

Note: HMTA - hexamethylenetetramine. Total S by elemental analysis. Free S determined by Soxhlet extraction with toluene (8 h). Bound S = total S - free S.

Soxhlet extraction with toluene (Section 2.4) was used to quantify unreacted elemental sulfur. For the SCC synthesized without catalyst, the free sulfur content was 12.3 ± 0.8 wt%, whereas the catalyst-containing SCC contained only 6.1 ± 0.5 wt% free sulfur. Correspondingly, the bound sulfur content (by elemental analysis after extraction) increased from 31.2 wt% to 38.4 wt% when the catalyst was used. These results directly demonstrate that hexamethylenetetramine promotes the incorporation of sulfur into the cellulose network, reducing the amount of residual elemental sulfur.

The observed increase in yield (by 6.6%), thermal stability (ΔT_{onset} = +24°C), and fluid loss reduction (by 14.2%) upon addition of 1 wt% hexamethylenetetramine is consistent with a nucleophilic initiation mechanism. The tertiary amine groups of urotropine may facilitate the ring-opening of S_8 at lower temperatures, generating more reactive polysulfide anions or radicals that react readily with cellulose hydroxyl groups. However, direct mechanistic evidence (e.g., by in situ Raman or electron paramagnetic resonance) is lacking; therefore, the proposed role remains hypothetical and requires further investigation.

Table 4

Fluid loss reduction and thermal stability of SCC vs. commercial additives

Additive (2 wt%)	Fluid loss reduction after aging* (%)	T_{onset} (°C)
CMC (LV grade)	12 ± 3	~190
PAC (HV grade)	35 ± 4	~210
Modified starch	8 ± 2	~175
SCC (this work, with catalyst)	62.5 ± 1.5	272

Hydrothermal aging at 180°C for 16 h in 3% KCl, 3% bentonite, pH 9.5-10.0. Fluid loss reduction relative to base fluid without additive.

For comparison, commercial fluid loss reducers - carboxymethyl cellulose (CMC, LV grade), polyanionic cellulose (PAC, HV grade), and modified starch - were tested at the same concentration (2 wt%) under identical conditions (3% bentonite, 3% KCl, pH 9.5-10.0). After hydrothermal aging at 180°C for 16 h, CMC and modified starch lost most of their effectiveness (fluid loss reduction <15%). PAC retained moderate activity (~35%), but its onset decomposition temperature ($T_{onset} \approx$ 210°C) indicates significant degradation. In contrast, SCC exhibited a fluid loss reduction of 62.5% after the same aging protocol, and its T_{onset} of 272°C is considerably higher than that of the commercial polymers. This makes SCC a promising thermostable additive for HTHP drilling fluids.

The dominant effect of temperature on all responses is explained by the kinetics of S_8 ring opening. Below 170°C, the concentration of active sulfur species is insufficient for deep copolymerization. At 185°C, the reaction reaches a balance between polymerization and depolymerization, giving maximum crosslink density. The optimum S:Org ratio of 55:45 reflects a trade-off: excess sulfur (S:Org > 60:40) leads to hydrophobicity and poor dispersion in water-based fluids, while excess cellulose (S:Org < 50:50) reduces thermal stability due to insufficient crosslinking.

The synthesized SCC meets the requirements for drilling fluid additives up to 180°C. However, the following limitations should be acknowledged: hydrothermal aging tests were performed only at 180°C for 16 h - longer durations and higher salinities (e.g., >3% KCl or seawater) were not tested; the exact chemical nature of the sulfur-cellulose linkage (thioether vs. physical entrapment) remains unconfirmed without XPS or solid-state NMR; benchmarking against commercial products was limited to fluid loss and TGA, not including rheological compatibility under dynamic HTHP conditions; the dispersion behavior and particle size effects on filtration performance were not systematically studied. Future work should address these aspects.

Conclusion

This study has established quantitative relationships between the key parameters of inverse vulcanization (temperature, time, and S:Org mass ratio) and the properties of sulfur-cellulose composites synthesized from waste elemental sulfur and activated cotton husk. The following conclusions are drawn:

A three-factor Box-Behnken design produced adequate regression models ($R^2 \geq 0.945$) for product yield, onset decomposition temperature, and fluid loss reduction efficiency. The dominant factor is temperature, followed by the S:Org ratio and, to a lesser extent, reaction time. The optimal conditions were: T = 185°C, τ = 135 min, S:Org = 55:45, giving a yield of 91.8%, T_{onset} = 272°C, and a fluid loss reduction of 62.5%, respectively (overall desirability D = 0.89).

FTIR spectroscopy revealed a band at 420 cm^{-1} (C-S) and the absence of an S-S band at 470-500 cm^{-1}, suggesting the formation of thioether linkages rather than long polysulfide chains. XRD showed only weak residual crystalline sulfur peaks, and SEM-EDX demonstrated homogeneous dispersion of sulfur within the cellulose matrix. Soxhlet extraction confirmed that the catalyst reduces free sulfur from 12.3% to 6.1%, directly proving increased chemical incorporation of sulfur.

Hexamethylenetetramine (1 wt% relative to sulfur) increases yield by 6.6%, thermal stability by 24°C, and fluid loss reduction by 14.2%, respectively. The proposed nucleophilic initiation mechanism remains hypothetical and requires further direct evidence (e.g., in situ spectroscopy).

The optimized SCC outperforms commercial additives (CMC, PAC, modified starch) in both thermal stability (T_{onset} = 272°C vs. ≤210°C) and fluid loss reduction after hydrothermal aging at 180°C (62.5% vs. ≤35%). It is recommended as a thermostable additive for water-based drilling fluids under HTHP conditions up to 180°C.

This work does not address long-term hydrothermal aging (>16 h), higher salinities, dynamic rheological compatibility, or the exact nature of the sulfur-cellulose bond (XPS/solid-state NMR required). Future studies should focus on these aspects and on scaling up the synthesis using local waste (gas processing

REFERENCES

[1]. Caenn, R., Darley, H. C., & Gray, G. R. (2016). Composition and Properties of Drilling and Completion Fluids (7th ed.). Boston: Gulf Professional Publishing. 734 p.
[2]. Fink, J. (2021). Petroleum Engineers Guide to Oil Field Chemicals and Fluids (3rd ed.). Gulf Professional Publishing. 844 p.
[3]. Plank, J., Dugonjić-Bilić, F., & Al-Humaidi, A. (2014). Thermal Degradation and Performance of Cellulose Derivatives in High-Temperature High-Pressure Drilling Fluids. Journal of Petroleum Science and Engineering, 119, 54-61.
[4]. Li, J., McDonald, A. G., & Westermann, N. M. (2016). Thermal degradation kinetics and rheological stability of polyanionic cellulose and carboxymethyl cellulose under HTHP conditions. Carbohydrate Polymers, 151, 485-493.
[5]. Klemm, D., Philipp, B., Heinze, T., Heinze, U., & Wagenknecht, W. (1998). Comprehensive Cellulose Chemistry. Volume 2: Functionalization of Cellulose. Weinheim: Wiley-VCH. 390 p.
[6]. Roy, D., Semsarilar, M., Guthrie, J. T., & Perrier, S. (2009). Chemistry of cellulose grafting. Chemical Society Reviews, 38(7), 2046-2064.
[7]. Chalker, J. M., Worthington, M. J., Lundquist, N. A., & Gibson, C. T. (2019). Inverse vulcanization: From fundamental chemistry to applications. Polymer Chemistry, 10(10), 1164-1178.
[8]. Hasell, T., Parker, D. J., Jones, H. A., McAllister, T., & Cooper, A. I. (2016). High-yield inverse vulcanization of sulfur. Chemical Science, 7(3), 1899-1905.
[9]. Smith, J. A., Wu, X., Sullivan, N. M., & Hasell, T. (2020). Inverse vulcanization of sulfur with bio-derived co-monomers and agricultural waste. Green Chemistry, 22(11), 3410-3422.
[10]. Lundquist, N. A., Green, S. J., & Chalker, J. M. (2021). Polysulfide polymers from sulfur and plant oils: Synthesis, properties, and applications. Journal of Polymer Science, 59(14), 1421-1436.
[11]. State Committee of the Republic of Uzbekistan on Statistics. (2024). Statisticheskiy ezhegodnik Respubliki Uzbekistan (Statistical Yearbook of the Republic of Uzbekistan). Tashkent: Goskomstat. 450 p. (Section: Industry and textile waste). (In Russ.).
[12]. Mirzaev, A. A., & Karimov, Kh. T. (2022). Kompleksnaya pererabotka sery neftegazovykh mestorozhdeniy Uzbekistana (Comprehensive processing of sulfur from oil and gas fields of Uzbekistan). Uzbekskiy khimicheskiy zhurnal (Uzbek Chemical Journal), (3), 54-61. (In Russ.).
[13]. Yunusov, Kh. E., Sarymsakov, A. A., & Rashidova, S. Sh. (2021). Poluchenie i fiziko-khimicheskie svoystva aktivirovannoy tsellyulozy iz shelukhi semyan khlopchatnika (Preparation and physicochemical properties of activated cellulose from cotton seed hulls). Khimiya Rastitelnogo Syrya (Chemistry of Plant Raw Materials), (2), 45-52. (In Russ.).
[14]. Akhmedov, O. M., & Dzhalilov, A. T. (2023). Termostabilnye polimernye kompozitsii na osnove mestnogo syrya i tekhnogennykh otkhodov (Thermostable polymer compositions based on local raw materials and industrial waste). Uzbekistan Journal of Polymers, 2(1), 18-25. (In Russ.).
[15]. Turabdzhanov, S. M., & Sharipov, M. S. (2024). Modifitsirovannye funktsionalnye kompozity dlya burovykh rastvorov glubokogo bureniya (Modified functional composites for deep drilling fluids). Uzbekistan Journal of Polymers, 3(2), 34-41. (In Russ.).
[16]. GOST 127.1-93. (1994). Sera tekhnicheskaya prirodnaya zhidkaya. Tekhnicheskie usloviya (Technical natural liquid sulfur. Specifications). Moscow: Izdatelstvo Standartov. 12 p.
[17]. GOST 4328-77. (1978). Reaktivy. Natriya gidrookis. Tekhnicheskie usloviya (Reagents. Sodium hydroxide. Specifications). Moscow: Izdatelstvo Standartov. 16 p.
[18]. GOST 3118-77. (1978). Reaktivy. Kislota solyanaya. Tekhnicheskie usloviya (Reagents. Hydrochloric acid. Specifications). Moscow: Izdatelstvo Standartov. 22 p.
[19]. GOST 6709-72. (1973). Voda distillirovannaya. Tekhnicheskie usloviya (Distilled water. Specifications). Moscow: Izdatelstvo Standartov. 8 p.

[20]. GOST 1381-73. (1974). Urotropin tekhnicheskiy (Geksametilentetramin). Tekhnicheskie usloviya (Technical urotropine (Hexamethylenetetramine). Specifications). Moscow: Izdatelstvo Standartov. 14 p.
[21]. GOST 28177-89. (1990). Glinoporoshki burovye bentonitovye. Tekhnicheskie usloviya (Bentonite clay powders for drilling fluids. Specifications). Moscow: Izdatelstvo Standartov. 18 p.
[22]. GOST 6840-78. (1979). Tsellyuloza. Metod opredeleniya soderzhaniya alfa-tsellyulozy (Cellulose. Method for determination of alpha-cellulose content). Moscow: Izdatelstvo Standartov. 10 p.
[23]. GOST 3584-73. (1974). Setki provolochnye tkanye s kvadratnymi yacheykami. Tekhnicheskie usloviya (Woven wire cloth with square openings. Specifications). Moscow: Izdatelstvo Standartov. 25 p.
[24]. Vogel, A. I. (2000). Vogels Textbook of Quantitative Chemical Analysis (6th ed. / revised by J. Mendham, R. C. Denney, J. D. Barnes, M. J. K. Thomas). London: Prentice Hall. 832 p.
[25]. EuroVector Instruments. (2018). CHNS-O Elemental Analyzer EA3000: User Manual and Operating Protocol. Pavia: EuroVector S.p.A. 112 p.
[26]. Shimadzu Corporation. (2016). LabSolutions IR Software Operation Manual: Fourier Transform Infrared Spectrophotometer. Kyoto: Shimadzu. 145 p.
[27]. International Centre for Diffraction Data (ICDD). (2023). Powder Diffraction File (PDF-2), Release 2023. Newtown Square, PA: ICDD.
[28]. JEOL Ltd. (2015). JSM-IT300 InTouchScope Scanning Electron Microscope: Operation Manual. Tokyo: JEOL. 210 p.
[29]. GOST R 56721-2015. (2016). Plastmassy. Termogravimetriya polimerov. Chast 1. Obshchie printsipy (Plastics. Thermogravimetry of polymers. Part 1. General principles (Determination of onset decomposition temperature T_{onset})). Moscow: Standartinform. 14 p.
[30]. API Recommended Practice 13B-1. (2019). Recommended Practice for Field Testing Water-based Drilling Fluids (5th ed.). Washington, D.C.: American Petroleum Institute. 132 p.
[31]. FANN Instrument Company. (2018). Instruction Manual: Model 35 6-Speed Rotational Viscometer. Houston: Fann Instrument Company. 68 p.